# Mechanical Stiffness Prediction of Beam-to-Column Stiffened Angle Joints

J. M. Reinosa*, A. Loureiro, R. Gutierrez and M. Lopez

Laboratorio de Análisis Estructural

Centro de Investigacións Tecnolóxicas (CIT)

Dpto. de Enxeñería Naval e Industrial

Universidade da Coruña (EPS Ferrol)

Mendizábal s/n Campus de Esteiro 15471 Ferrol, Spain

*Corresponding author. E-mail: jreinosa@udc.es. Tel.: +34 981167000x3297. Fax: +34 981337410

This is a post-peer-review, pre-copyedit version of an article published in the Journal of Constructional Steel Research. The final authenticated version is available online at: https://doi.org/10.1016/j.jcsr.2019.105875.



## Abstract

Semi-rigid angle joints, in their different configurations, constitute a highly interesting alternative to other typologies like end plate joints. However, they are not widely used in the customary practice of European steel construction. The assembly of these joints is simple and cost effective, and they are a good choice in deconstruction and seismic designs. The stiffness of cleat angle joints can be increased either by preloading the bolts or by adding stiffeners to the angles. The development of theoretical models to evaluate both the stiffness and the resistance of these joints depends essentially on the existence of sufficient experimental evidence to validate them. Although there is already a reasonable number of tests on semi-rigid angle joints, this is not so in the case of joints with stiffened angles. Therefore, this study displays the results of experiments consisting of eight tests on stiffened angle joints. Moreover, an analytical model to predict the rotational stiffness, based on the Eurocode 3 Component Method according to a non-aligned model, is proposed. In this approach, a previously developed plate model is introduced to assess the axial stiffness of the top angle in bending. In addition, a new component that takes into account the stiffener in compression is presented. The proposed methodology is successfully validated with tests from the experimental work, as well as with previous tests from other researchers.

**Keywords:** Angle joints; Rotational stiffness; Semi-rigid joints; Experimental study

## 1. Introduction

The use of bolted connections in steel construction has gradually been replaced by welding, especially since the mid-20$^{th}$ century, due to the invention of flux-cored and plasma arc welding, which resulted in greatly increased welding speeds. The decision between bolting or welding depends largely on the nature of the structure and the resources of the contractors. From a construction standpoint, welding is a skilled labour and it has a very high set-up cost. In addition, accessibility is an issue and it is difficult to certify or inspect. Moreover, welded connection delays may arise from the absence of a qualified welder, welding platforms or cold windy weather. In contrast, bolted connections have cost advantages because drilling or punching of bolt holes or cutting of the material are often carried out by computed numerical control machines [1]. Furthermore, bolted connections are quicker to erect, thereby leading to shorter construction times.

The top and seat angle connection with a double-web angle is one of the most common semi-rigid bolted typologies in North America. This connection usually exhibits high ductility and is therefore more suitable for seismic design than welded moment connections, which did not perform adequately during the last major seismic events [2]. Bolted angle connections possess sufficient ability to suit adjustments in situ during erection and they are easier to take apart without damage to the steel than welded connections, thereby preserving the independence of the members and improving deconstructability and reusability [3, 4]. On this basis, although design for deconstruction requirements go beyond technical competencies and non-technical factors, such as stringent legislation and policy and design processes and competency for deconstruction, are key in designing deconstructable buildings, welds tend to exhibit brittle failure and therefore, in the case of disassembly, a crane that supports the beam throughout weld removal will be necessary.

Despite their many advantages, angle connections lack the ability to meet rolling tolerances in beams and can become inconvenient if accessories intrude into the space above and below the beam. In the case of reuse, a drilled steel member may not be reusable until the old holes are patched. Their lack of usage in the European steelwork sector may also be due to the complexity involved in its calculation from the perspective of the Component Method [5]. Therefore, the proposal of simplified analytical

methodologies that are suitable for simple calculations or are easily programmable can help to overcome this obstacle.

Although this typology appears in the Eurocodes [5], it has not been as developed as other typologies, such as end plate joints. Nevertheless, in recent years, numerous theoretical and numerical proposals have emerged, some of which are relatively simple, which adapt to the Component Method and allow us to approximate both the stiffness and resistance of this type of joint. Azizinamini et al. [6] proposed a simple analytical method to predict the initial rotational stiffness disregarding the column components. Faella et al. [7] developed a model that includes the panel zone and improves upon previous approaches. Furthermore, in line with the previous proposal, a frame approach for the rotational stiffness estimation of preloading and non-preloading cleat angle joints was developed [8,9]. In contrast, Lemonis and Gantes [10] designed advanced mechanical models designed that are programmable. Furthermore, finite element proposals were developed [11], albeit with the inconvenience of the great effort required for the development of the models and the high computational costs.

The stiffness of angle joints can be increased either by preloading the bolts or by adding stiffeners to the angles. Some recent articles have reported the stiffening of angle cleats and make some interesting proposals for the determination of their mechanical characteristics [12–14]. However, in order to validate certain proposed models, it is advisable to have a reasonable number of experimental tests. The number of tests regarding joints with stiffened angles in the literature is limited [12,15,16] and for this reason, one of the objectives of this work is to provide a series of tests that help to contrast the different proposals. We consider eight angle joints in this study. A second objective of this study is the inclusion in the Component Method of a proposal to estimate the axial stiffness of stiffened angle cleats based on a plate approach [13]. This axial stiffness will therefore be introduced as the component top angle in bending, following a non-aligned model similar to that used by Faella et al. [7], which has proven to be very effective at other times for estimating the rotational stiffness. The methodology will be contrasted with the tests developed in the present study and also with other existing tests in the literature, such as those by Skejic et al. [12] and Ghindea et al. [15].

## 2. Experimental evidence from literature

*2.1 Experimental campaign from Skejic et al.*

Skejic et al. developed a well-documented experimental campaign, with four duplicate tests on semi-rigid cleat angle joints. Three of them contain stiffened angles in different configurations: test series *B* (tests *B1* and *B2*), *C* (tests *C1* and *C2*) and *D* (tests *D1* and *D2*). Figure 1 shows the arrangement and basic geometrical characteristics of these tests. The top angle is the angle in tension and the seat angle is the angle in compression. The column and beam were selected so that they remained undamaged during the tests. The angles are L150.90.10 and the column was selected as extremely rigid, so the panel components do not contribute to the joint rotational stiffness.

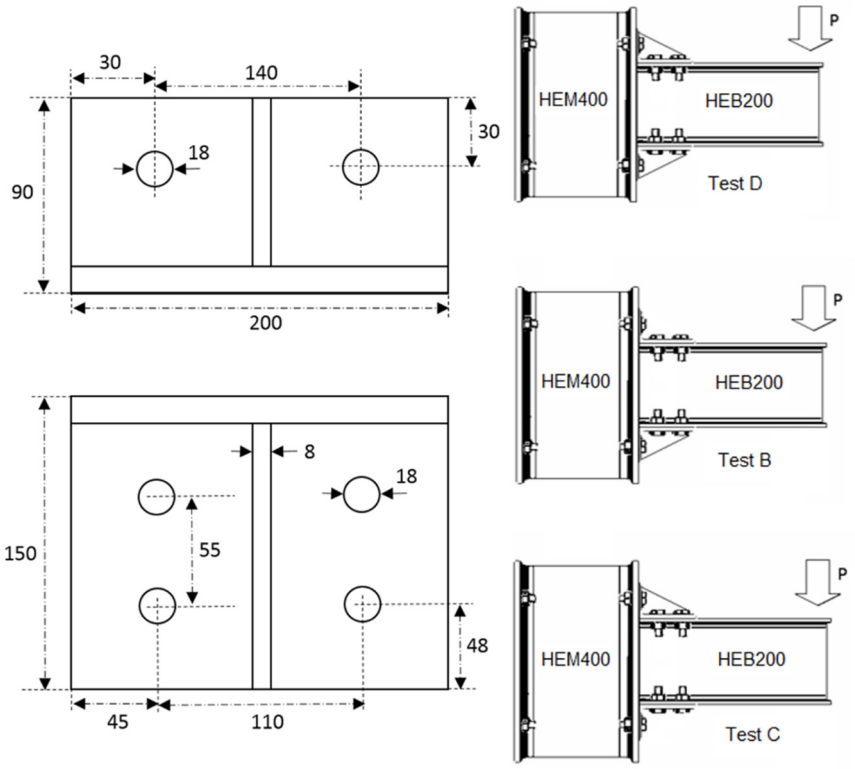


*Figure 1. Stiffened angle joint tests from Skejic et al. Dimensions given in mm.*

More details regarding this experimental study can be found in [12].

*2.2 Experimental study of Ghindea et al.*

Ghindea et al. carried out an experimental study consisting of four tests on angle joints, two of them including stiffened angles: test *TSDWS-10* (top and seat with double-web angle; stiffened top angle; 10 mm thick) and test *TSS-10* (top and seat angle; stiffened top angle; 10 mm thick). The top angle is the angle in tension and the seat angle is the angle

in compression. The basic geometry and configuration of the specimens replicate a previous test of an unstiffened angle joint [17] but considering stiffened L120.90.10 top and seat angles. Figure 2 shows these joints, which will be also used to validate the proposed methodology.

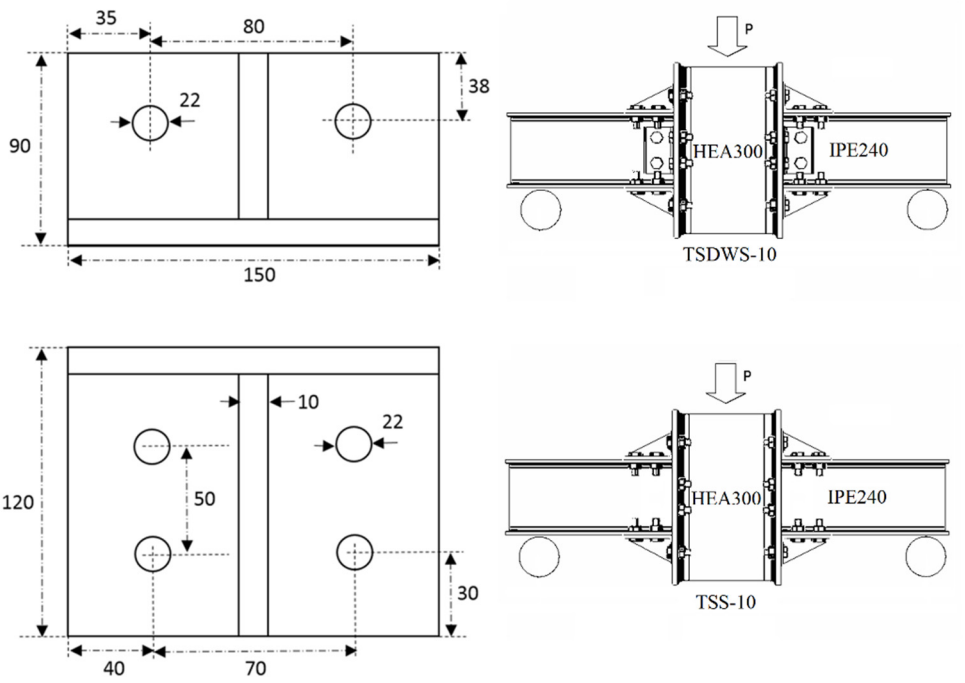


*Figure 2. Stiffened angle joint tests from Ghindea et al. Dimensions in mm.*

More information regarding the experimental work from Ghindea et al. can be found in [15].

## 3. Experimental study

As discussed, the validation of a mechanical model, which is the final objective of this study, requires experimental data. Thus, an experimental study on joints with stiffened angles has been developed to complement the sources of testing that has just been described. This experimental campaign was carried out in the LAE (Structural Analysis Lab) of the Industrial Engineering School in the University of A Coruña. In this section, the experimental work is described. Finally, the experimental results are analysed.

### *3.1. Setup of tests*

Eight tests on joints with stiffened angles have been carried out and designated as ***S****(stiffened)****T****(test)* + *test number*. Figure 3 and Table 1 show the different tested typologies and

configurations. The top angle is the angle in tension and the seat angle is the angle in compression. The morphology of the tests consisted basically of two HEB 240 beams joined to a HEA 300 column through stiffened top and seat angle joints with double-web angles, except tests *ST6–ST8*, which lack web angles. Test *ST6* has stiffened top and seat angles. On the other side, in test *ST7*, only the seat angle is stiffened. In addition, in test *ST8*, only the top angle is stiffened. The gap between the beam and column flange in the experimental work was ~2 mm in all specimens. Table 2 shows the mechanical properties of the specimen members, namely, yield stress, ultimate stress and ultimate strain. A *System 7000* scanner and a *StrainSmart*® data acquisition system were used for the experimental measurements. The beams were simply supported and the load was applied as shown in Figures 3 and 4, thus the top angle is the one below. Snug-tighten M20 10.9 bolts and L100.10 web angles were used. Furthermore, L120.90.*t* top and seat angles were selected, where *t* represents the angle thickness shown in Table 1. The sub-index ***s*** in Table 1 reports if the angle is stiffened or not in each test. The stiffener thickness was 10 mm in all cases. The bolt hole layout in the top and seat angles is the same as in [17] and also in Ghindea's tests, as shown in Figure 2. There were no significant differences between the nominal and the actual values of the angle thickness.

| Test | TOP ANGLE | SEAT ANGLE | WEB ANGLE |
|---|---|---|---|
| ST1 | 8S | 8S | 10 |
| ST2 | 9S | 9S | 10 |
| ST3 | 10S | 10S | 10 |
| ST4 | 9S | 10S | 10 |
| ST5 | 8S | 10S | 10 |
| ST6 | 8S | 10S | -- |
| ST7 | 8 | 10S | -- |
| ST8 | 10S | 10 | -- |

*Table 1. Angle thickness (mm) and stiffener presence indicator.*

| Element | fy (MPa) | fu (MPa) | Extension (%) |
|---|---|---|---|
| L150.90.8 | 349 | 474 | 28.0 |
| L150.90.9 | 353 | 479 | 26.1 |
| L150.90.10 | 346 | 473 | 29.0 |
| Stiffener | 349 | 498 | 27.5 |
| HEA 300 | 435 | 617 | 26.4 |
| HEB 240 | 447 | 625 | 28.2 |

*Table 2. Mechanical properties of laminates.*

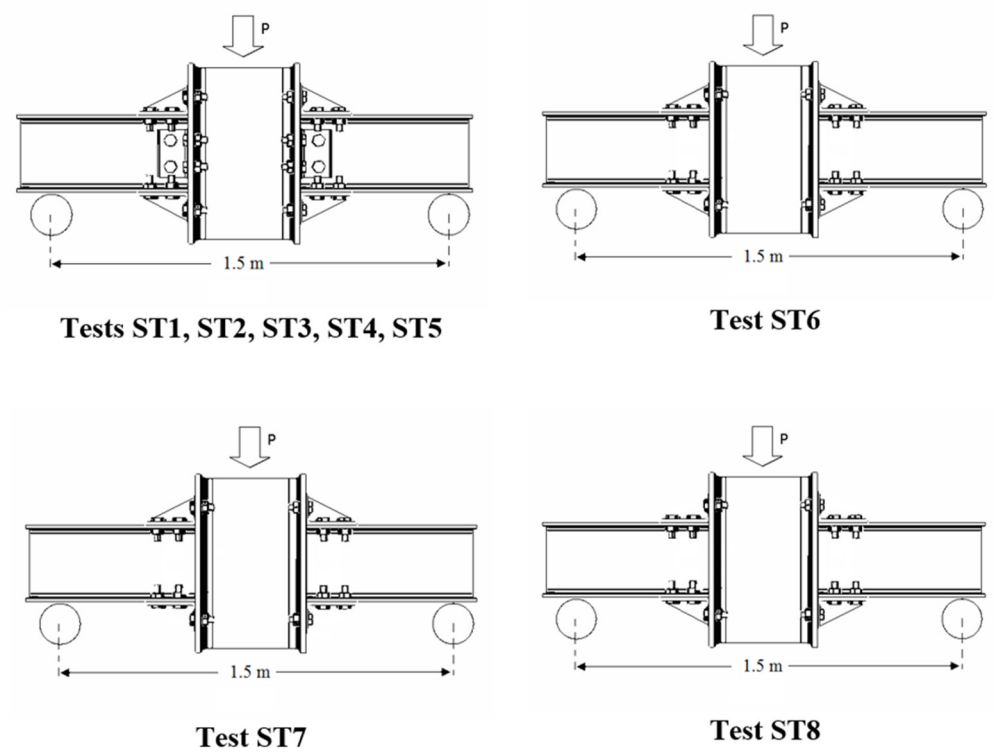


*Figure 3. Test configurations for the experimental campaign.*

The load cell and actuator are located in the top of the column and they both have a capacity of 300 kN. The beam rotation was monitored through two inclinometers placed on the top of the beams, close to the seat angles. Finally, a wire sensor was located in the base of the column to obtain additional measures. High-level cards were used for inclinometers and strain gage cards for the load cell and the wire sensor. Figure 4 shows the measurement device setup. A preloading step was accomplished in the elastic range for each test.

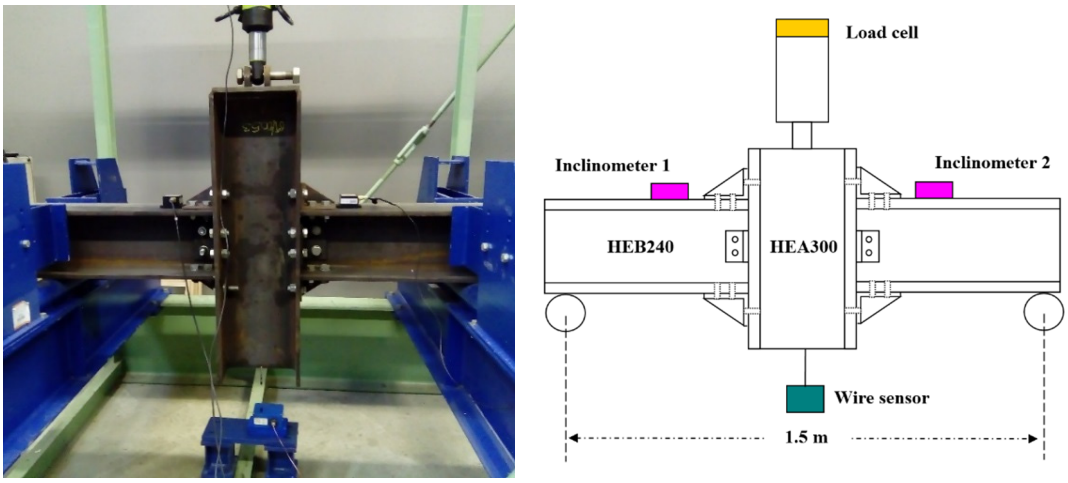


*Figure 4. ST1 test arrangement.*

*3.2 Test results*

Figure 5 shows the original and deformed configurations for tests *ST3* and *ST7*, with and without web angles, respectively. The moment-rotation (MR) curves were obtained through a fitting process from the average measures of the right (+) and left (-) beam rotations. The rotation was directly measured by the inclinometers: inclinometer 1 measured the rotation in the left side of the joint and inclinometer 2 measured the rotation in the right side of the joint, as shown by Figure 4. The relative rotation between the right and left sides was controlled to verify the symmetry condition. Figure 6 shows the complete MR curve before the fitting process for *ST4* test and the relative rotation along the test execution. The level of distortion was generally very low for all specimens.

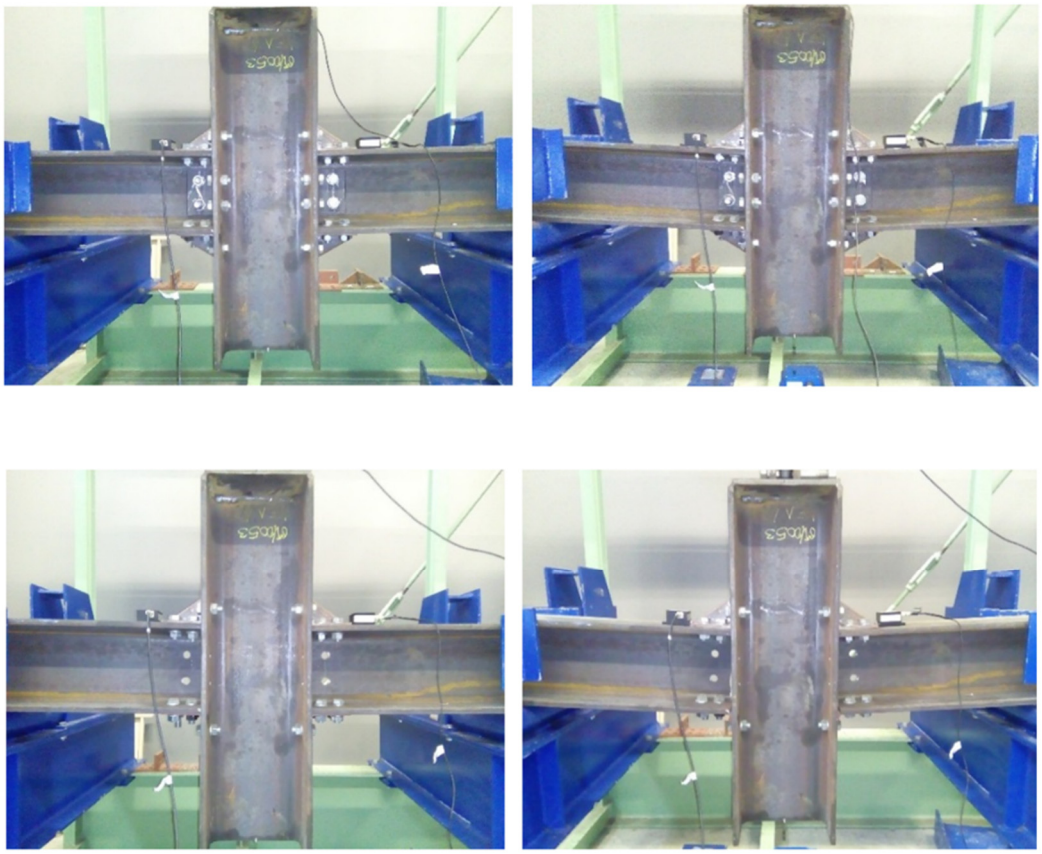

*Figure 5. ST3 (top) and ST7 (bottom) original and deformed configurations.*

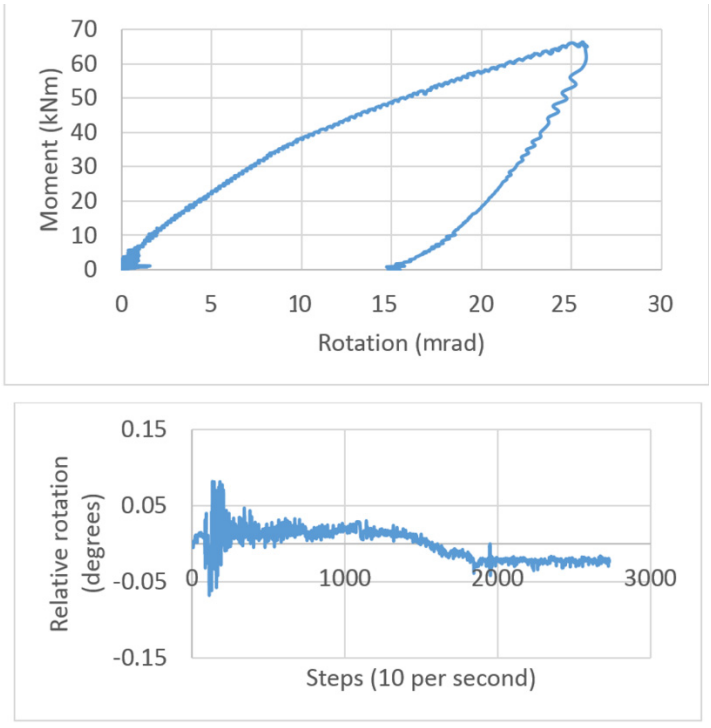


*Figure 6. MR curve before fitting for ST4 test and relative rotation.*

The stiffness values before and after the knee range are computed by means of linear regression analysis of the quasi-linear branches representing the elastic and post-critical behaviour, respectively. The bending resistance $M_{Rd}$ was determined at the intersection of these fitted lines, which define the initial and post-yielding stiffness. Figure 7 shows this procedure for the *ST6* test.

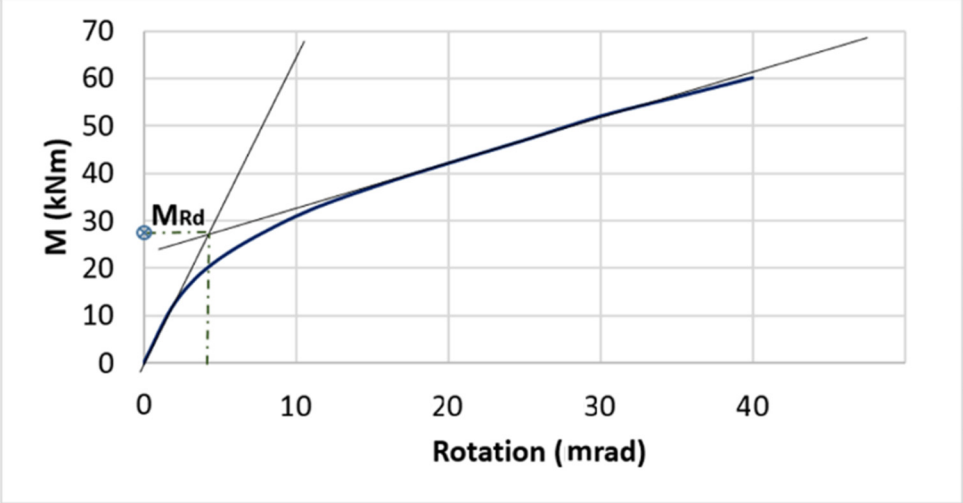


*Figure 7. Determination of resistance moment for ST6 test.*

Table 3 displays the experimental initial stiffness and resistance results for all specimens, where "+" denotes the value on the right side, "-" denotes the value on the left side of the joint and the third value is the average of the two preceding values regarding both stiffness and resistance.

| Specimen | $S_{jini+}$ (kNm/rad) | $S_{jini-}$ (kNm/rad) | $S_{jini}$ (kNm/rad) | $M_{jRd+}$ (kNm) | $M_{jRd-}$ (kNm) | $M_{jRd}$ (kNm) |
|---|---|---|---|---|---|---|
| ST1 | 6021 | 6383 | **6202** | 38.17 | 37.44 | **37.81** |
| ST2 | 6598 | 6742 | **6670** | 40.89 | 38.64 | **39.76** |
| ST3 | 7244 | 7456 | **7350** | 43.26 | 45.32 | **44.29** |
| ST4 | 6750 | 6856 | **6803** | 43.71 | 43.95 | **43.83** |
| ST5 | 6360 | 6504 | **6432** | 30.56 | 31.12 | **30.84** |
| ST6 | 5338 | 5550 | **5444** | 26.89 | 32.38 | **29.63** |
| ST7 | 4486 | 4604 | **4545** | 14.54 | 14.95 | **14.74** |
| ST8 | 5391 | 5569 | **5480** | 41.35 | 42.18 | **41.76** |

*Table 3. Experimental rotational stiffness and resistance moments.*

Figure 8 shows the comparison between the MR curves of tests *ST1* to *ST3*, where the top and seat stiffened angle thickness is 8 mm in test *ST1*, 9 mm in test *ST2* and 10 mm in test *ST3*. The stiffness of test *ST2* is 7.5% higher than that of *ST1* and the stiffness of test *ST3* is about 10% higher than that of *ST2*.

Figure 9 compares the results of tests *ST5*, *ST6* and *ST7*, where the seat stiffened angle is the same but the configurations of the top and web angles are different. Tests *ST6* and *ST7* do not have web angles and *ST7* nor stiffener in the top angle. The difference in stiffness between tests *ST5* and *ST6* (without web angles) is ~18% and when the comparison is established between tests *ST6* and *ST7*, the difference reaches 16.5%.

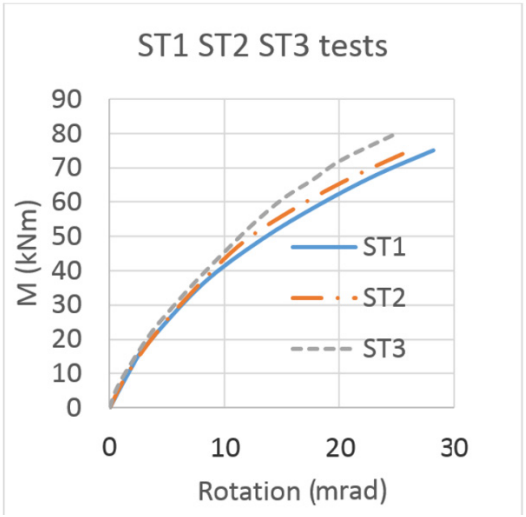


| Test | TOP ANGLE | SEAT ANGLE | WEB ANGLE |
|---|---|---|---|
| ST1 | 8 S | 8 S | 10 |
| ST2 | 9 S | 9 S | 10 |
| ST3 | 10 S | 10 S | 10 |

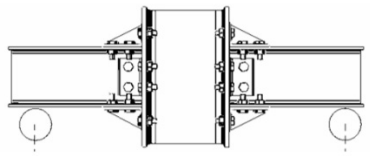

*Figure 8. ST1, ST2 and ST3 MR curves.*

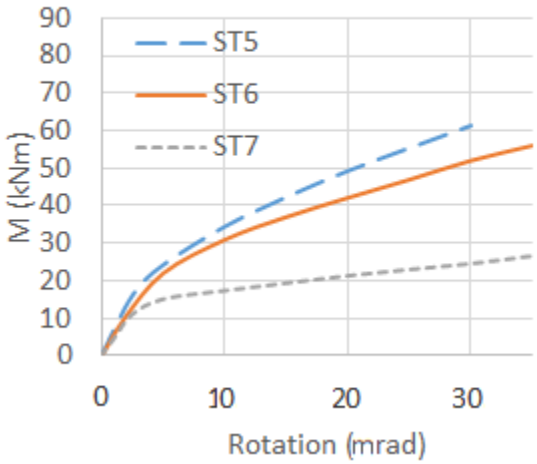


| Test | TOP ANGLE | SEAT ANGLE | WEB ANGLE |
|---|---|---|---|
| ST5 | 8 S | 10 S | 10 |
| ST6 | 8 S | 10 S | -- |
| ST7 | 8 | 10 S | -- |

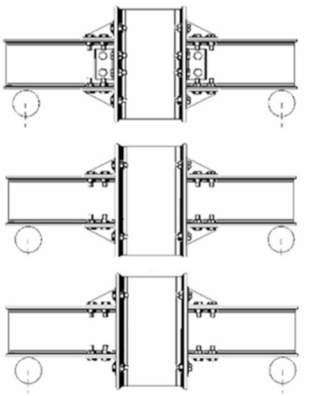

*Figure 9. ST5, ST6 and ST7 MR curves.*

Figure 10 compares the isolated effect of the stiffened top angle thickness by showing the experimental MR curves of tests *ST3*, *ST4* and *ST5* (10, 9 and 8 mm thick, respectively), all of them with a stiffened seat angle that is 10 mm thick. The differences in stiffness and resistance between tests *ST3* and *ST5* are 12.5% and 44%, respectively. These results indicate the relevance of the stiffened top angle thickness as far as resistance is concerned.

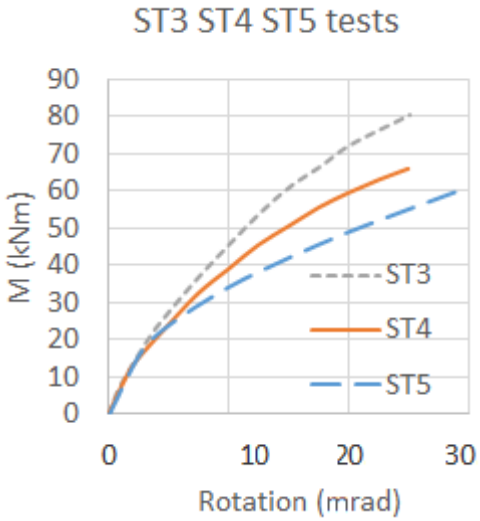


| Test | TOP ANGLE | SEAT ANGLE | WEB ANGLE |
|---|---|---|---|
| ST3 | 10 S | 10 S | 10 |
| ST4 | 9 S | 10 S | 10 |
| ST5 | 8 S | 10 S | 10 |

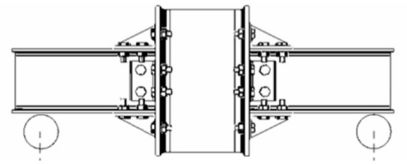

*Figure 10. ST3, ST4 and ST5 MR curves.*

Finally, Figure 11 compares tests *ST3* and *ST8* (this one without web angle and with unstiffened seat angles). The stiffness of test *ST3* (stiffened seat angle) is ~34% higher than the stiffness of *ST8* test.

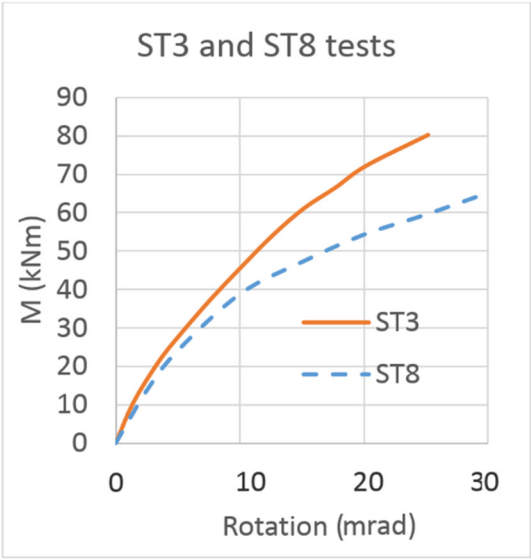


| Test | TOP ANGLE | SEAT ANGLE | WEB ANGLE |
|---|---|---|---|
| ST3 | 10 S | 10 S | 10 |
| ST8 | 10 S | 10 | -- |

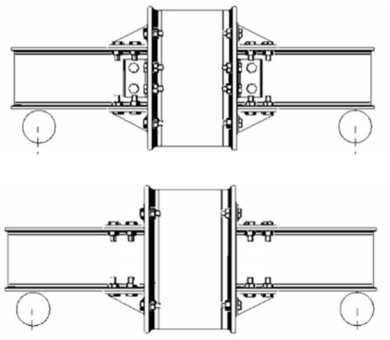

*Figure 11. ST3 and ST8 MR curves.*

In Figure 12, the deformed top angles of the *ST4* test are shown. The three-dimensional nature of deformation can be observed in this figure. This deformational behaviour was the main reason for adopting a plate model for modelling the axial stiffness of the component stiffened angle in bending [13], as discussed in the next section. The only remarkable event during the experimental work was a sudden weld failure in the *ST2* test that occurred after the short angle leg yielding.

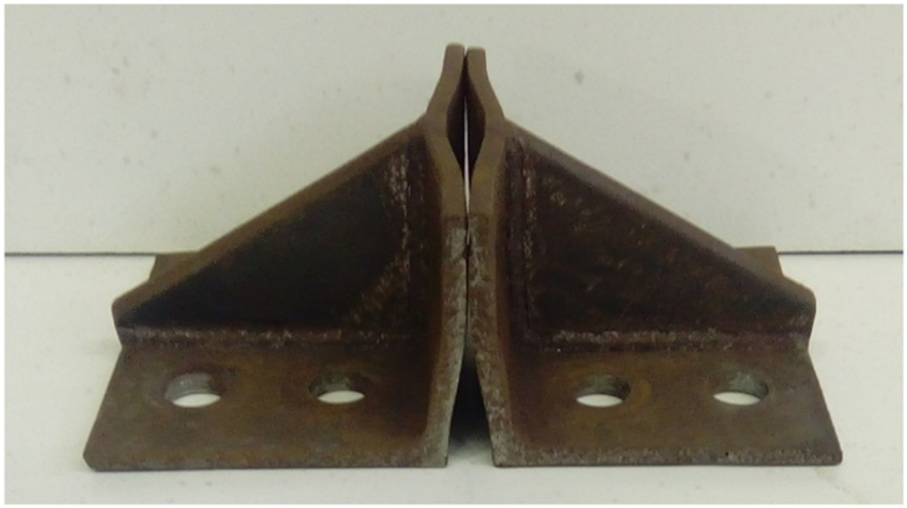

*Figure 12. Top angle deformation for ST4 test.*

## 4. Plate model for predicting axial stiffness of top stiffened angles in bending

In [13], a plate model for the prediction of the axial stiffness of stiffened cleat angles was proposed and validated. Additionally, an effective width for stiffness calculations was defined. The stiffness concerning this problem resulted in:

$$K_0 = \frac{F}{w_{\max}} = \frac{D}{\eta m^2} \tag{1}$$

where $F$ is the force, $w_{max}$ is the maximum deflection, $\eta$ is a deflection parameter, $m$ is the distance between the yielding lines, as shown in Figure 13, and $D$ is the flexural stiffness of the plate, defined as follows:

$$D = \frac{E t_a^3}{12(1-\vartheta^2)} \tag{2}$$

where $t_a$ is the thickness of the angle.

The parameter $\eta$ was defined as:

$$\eta\left(\frac{t_a}{m}\right) = ae^{\left(\frac{bt_a}{m}\right)} \quad (3)$$

where parameters *a* and *b* were calculated by:

$$a(\beta) = a_1 ln(\beta) + a_2 \quad (4)$$

$$b(\beta) = b_1\beta^{b_2} + b_3 \quad (5)$$

$$a_1 = -0.003t_a + 0.2772 \quad (6)$$

$$a_2 = 0.266 \quad (7)$$

$$b_1 = 0.4825 \quad (8)$$

$$b_2 = -1.665 \quad (9)$$

$$b_3 = 1.08 \quad (10)$$

The dimensionless parameter $\beta$ was defined as:

$$\beta = \frac{d}{m} \quad (11)$$

An equivalent $d_{eq}$ parameter, shown in Figure 13, was proposed to include the prying and bolting effects:

$$d_{eq} = d\left[\alpha(d)\frac{m}{b_a} + \beta(d, t_a)\right] \quad (12)$$

where

$$\beta(d, t_a) = (-0.001d - 0.0016t_a + 0.0586) \quad (13)$$

$$\alpha(d) = [59d^{-1.266} + 0.371] \quad (14)$$

$$d = b_a - e_b - \frac{d_b}{2} \quad (15)$$

$$m = L - e_L - t_a - 0.8r - \frac{d_{bh}}{2} \quad (16)$$

The parameters $t_s$, $d_b$, $d_{bh}$ and $r$ were the thickness of the stiffener, the bolt diameter, the bolt head diameter and the angle root radius, respectively.

The effective width specifically proposed for the computation of stiffness is shown in Figure 14, where $m_{EC3}$ is the distance between yielding lines proposed by EC3 [5]. Additional information can be found in [13]. This approach will be later introduced in the mechanical model concerning the Component Method of Eurocode 3.

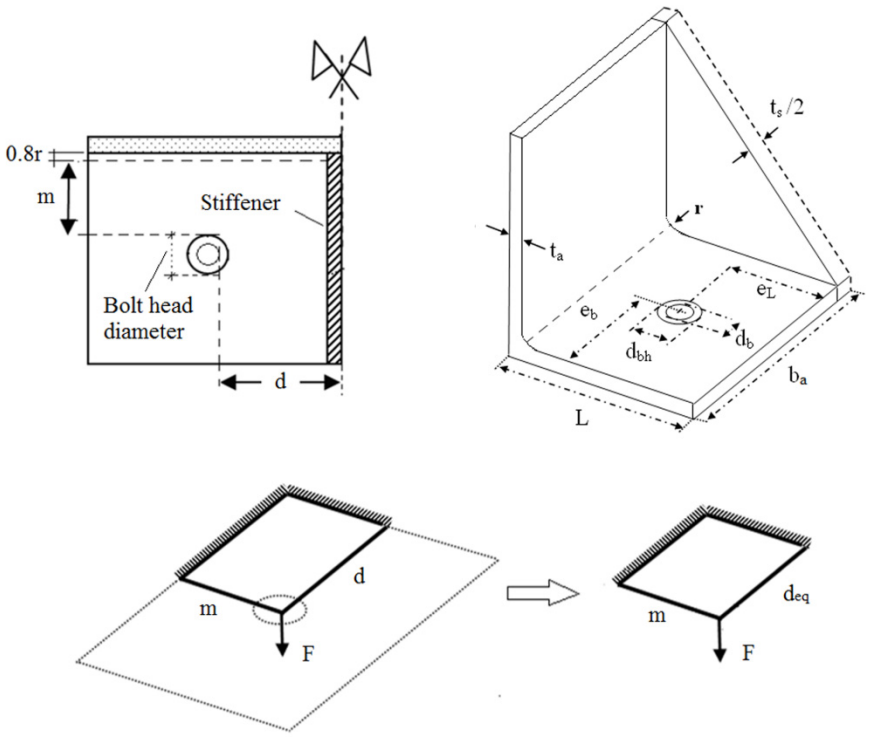


*Figure 13. Simplified plate model.*

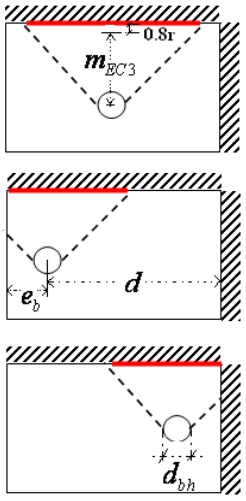


$$b_{eff} = 2m_{EC3} + d_{bh} \le b$$

$$b_{eff} = e_b + m_{EC3} + \frac{d_{bh}}{2} \le b \Leftrightarrow e_b < m_{EC3} + \frac{d_{bh}}{2}$$

$$b_{eff} = d + m_{EC3} + \frac{d_{bh}}{2} \le b \Leftrightarrow d < m_{EC3} + \frac{d_{bh}}{2}$$

*Figure 14. Effective width for stiffness calculations.*

## 5. New component development for stiffener in compression

The deformability of the seat angle stiffener in compression can be introduced in the Component Method. A simplified model considering the stiffener as a variable section bar is proposed. The bar dimensions are shown in Figure 15. The expression for the shortening is expressed as:

$$d\Delta = \frac{F_c dx}{EA(x)} = \frac{F_c dx}{E[h(x)t_s]} \tag{17}$$

where $D$ is the shortening due to the compression force $F_c$ and

$$h(x) = H_1 + \frac{[H_2 - H_1]}{L_s} x \tag{18}$$

Solving the integral through a change of variable:

$$\Delta = \int_{H_1}^{H_2} \frac{F_c L_s}{E t_s} \frac{d\theta}{\theta} = \frac{F_c L_s [ln(H_2) - ln(H_1)]}{E(H_2 - H_1) t_s} \tag{19}$$

Thus, the stiffness for the stiffener in compression results in:

$$K_{sc} = \frac{E(H_2 - H_1) t_s}{L_s [ln(H_2) - ln(H_1)]} \tag{20}$$

where $t_s$ is the stiffener thickness and $H_1$, $H_2$ and $L_s$ are the stiffener dimensions.

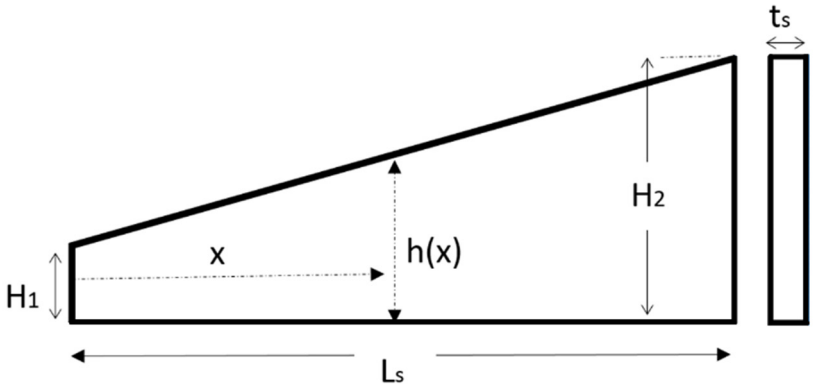


*Figure 15. Stiffener geometry.*

## 6. Rotational stiffness prediction

The methodology for the evaluation of the rotational stiffness of stiffened angle joints follows the process described by Eurocode 3 [5] and developed by Faella et al. [7] and also by the authors who predicted the rotational stiffness of unstiffened joints [9]. It follows a non-aligned model [10], where the springs representing the column panel components are lined with the bolt axis. In addition, the connection springs are lined with the angle leg, which is bolted to the beam. For the stiffness evaluation of each bolt row, $K_i^s$ will concern the bolt row stiffness of stiffened joints and $K_i$ will name the bolt row stiffness of unstiffened joints. An important difference with the method of Faella et al. [7] for unstiffened joints is the inclusion of the bolt in the frame approach, representing the top angle and the column flange in bending [9].

In this study, considering the three-dimensional nature of the stiffened angle deformation, we decided not to use the usual beam or frame models for the component stiffened angle in bending, and to follow a previously established proposal of a plate model that can be more suitable to represent a more complex deformational behaviour [13]. Therefore, when the top angle is stiffened, the top angle in bending will be simulated by means of the plate analogy, which does not include the bolt. Hence, in this case, the component bolt in tension must be introduced, but with the tributary length concerning the angles in bending. Nevertheless, the column flange in bending and web angles in bending are still represented through the frame approach [9].

The presented methodology, when the top angle is stiffened, considers four deformation sources in line with the top angle leg bolted to the top beam flange: top angle in bending, bolts in shear, top beam flange in bearing and top angle in bearing. These components contribution will be translated to the first bolt row through the following expressions [7]:

$$K_{ta}^{*} = K_{ta}\left(\frac{h_{ta}}{h_1}\right)^2 \tag{21}$$

$$K_{bs}^{*} = K_{bs}\left(\frac{h_{ta}}{h_1}\right)^2 \tag{22}$$

$$K_{bfb}^{*} = K_{bfb}\left(\frac{h_{ta}}{h_1}\right)^2 \tag{23}$$

$$K_{tab}^{*} = K_{tab}\left(\frac{h_{ta}}{h_1}\right)^2 \tag{24}$$

The notation and location of these components are shown in Figures 16 and 17. As Figure 17 shows, the parameter $h_{ta}$ is the lever arm of the top angle leg connected to the beam flange and $h_1$ is the lever arm for the first bolt row, measured from the centre of compression. Thus, the stiffness of the first bolt row, considering stiffened joints, is calculated as:

$$K_1^S = \frac{1}{\frac{1}{K_{cwt}}+\frac{1}{K_{cfb}}+\frac{1}{K_{bt}}+\frac{1}{K_{ta}^*}+\frac{1}{K_{bs}^*}+\frac{1}{K_{bfb}^*}+\frac{1}{K_{tab}^*}} \tag{25}$$

The stiffness of the bolt rows regarding the web angle, as shown in Figure 16, remains:

$$K_i^S = K_i = \frac{1}{\frac{1}{K_{cwt}}+\frac{1}{K_{cfb}}+\frac{1}{K_{wa}}+\frac{1}{K_{bs}}+\frac{1}{K_{bwb}}+\frac{1}{K_{wab}}} \tag{26}$$

where the coefficient $i$ changes from 2 to $n$ regarding the web angle rows.

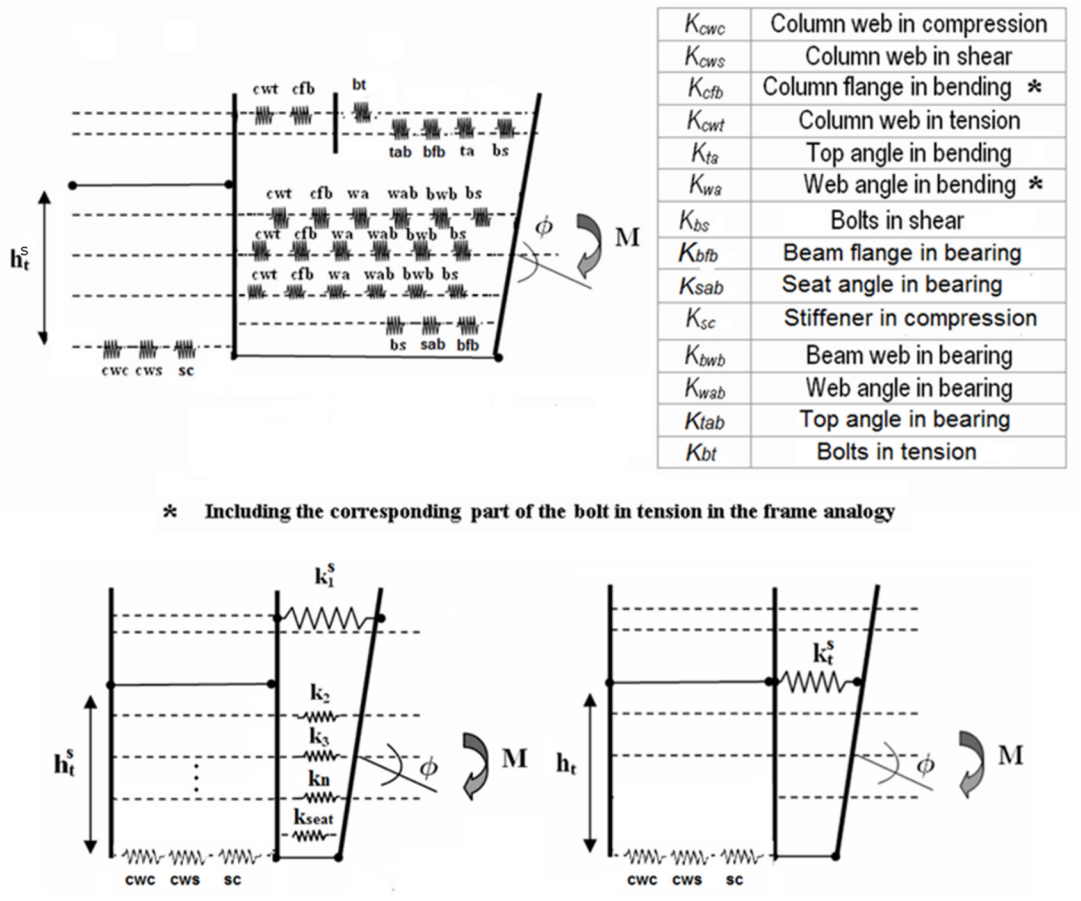


| | |
|---|---|
| $K_{cwc}$ | Column web in compression |
| $K_{cws}$ | Column web in shear |
| $K_{cfb}$ | Column flange in bending * |
| $K_{cwt}$ | Column web in tension |
| $K_{ta}$ | Top angle in bending |
| $K_{wa}$ | Web angle in bending * |
| $K_{bs}$ | Bolts in shear |
| $K_{bfb}$ | Beam flange in bearing |
| $K_{sab}$ | Seat angle in bearing |
| $K_{sc}$ | Stiffener in compression |
| $K_{bwb}$ | Beam web in bearing |
| $K_{wab}$ | Web angle in bearing |
| $K_{tab}$ | Top angle in bearing |
| $K_{bt}$ | Bolts in tension |

* Including the corresponding part of the bolt in tension in the frame analogy

*Figure 16. Proposed non-aligned mechanical model for stiffened TSDW angle joints.*

The centre of compression, when the seat angle is stiffened, is located considering the proposal of Skejic et al. [12] for the lever arm, thus it is placed at a distance of $d_{bh}/2$ from the seat angle bolt axis, where $d_{bh}$ is the bolt head diameter, as shown in Figure 17.

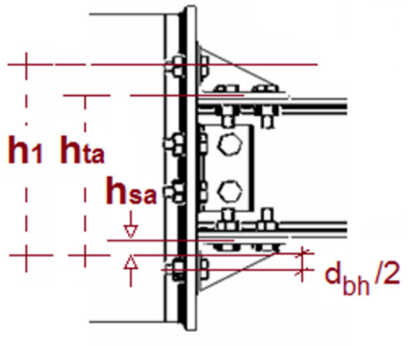


*Figure 17. Proposal of Skejic et al. for the lever arm in joints with a stiffened seat cleat.*

On this basis, the deformation sources regarding the seat angle leg and seat beam flange, namely, the bolts in shear, seat beam flange in bearing and seat angle in bearing, are considered with a lever arm $h_{sa}$. This stiffness coefficient is described by Eq. (27):

$$K_{seat} = \frac{1}{\frac{1}{K_{bs}}+\frac{1}{K_{sab}}+\frac{1}{K_{bfb}}} \tag{27}$$

The lever arm $h_t^S$ defined as the distance between the centre of compression and the resultant pull force location, can be calculated as:

$$h_t^s = \frac{\sum_{i=1}^{n} K_i^s h_i^2 + K_{seat}\, h_{sa}^2}{\sum_{i=1}^{n} K_i^s h_i + K_{seat}\, h_{sa}} \tag{28}$$

The parameter $h_i$ refers to the separation between the centre of compression and the $i^{th}$ bolt row. In addition, $n$ is the number of bolt rows connecting the angles to the column flange. The total inputs regarding the components that depend on the considered bolt row can be computed through a tantamount spring located at the tension centre. This equivalent stiffness is computed by:

$$K_t^s = \frac{\sum_{i=1}^{n} K_i^s h_i + K_{seat}\, h_{sa}}{h_t^s} \tag{29}$$

The total inputs of the components depending and not depending on the bolt rows, including the new component representing the stiffener in compression, can be combined to produce:

$$K_{\emptyset}^{s} = \frac{(h_t^s)^2}{\frac{1}{K_{cwc}}+\frac{1}{K_{cws}}+\frac{1}{K_t^s}+\frac{1}{K_{sc}}} \tag{30}$$

If the seat angle is not stiffened, the following expression must be used:

$$K_{\emptyset} = \frac{h_t^2}{\frac{1}{K_{cwc}}+\frac{1}{K_{cws}}+\frac{1}{K_t}+\frac{1}{K_{bs}}+\frac{1}{K_{sab}}+\frac{1}{K_{bfb}}} \tag{31}$$

where $K_{\phi}^{s}$ is the overall rotational stiffness for stiffened joints and $K_{\phi}$ is the overall rotational stiffness for unstiffened joints, where

$$K_t = \frac{\sum_{i=1}^{n} K_i h_i}{h_t} \tag{32}$$

$$h_t = \frac{\sum_{i=1}^{n} K_i h_i^2}{\sum_{i=1}^{n} K_i h_i} \tag{33}$$

A summary of the approaches considered for each component is shown in Table 4.

| | |
|---|---|
| **Top angle in bending (stiffened)** | Plate model [13] |
| **Top angle in bending (unstiffened)** | Frame model [8,9] |
| **Plates in bearing** | EC3 [5] |
| **Column flange in bending** | Frame model [8,9] |
| **Column web in tension** | Faella et al. [7] |
| **Column web in compression** | Faella et al. [7] |
| **Web angle in bending** | Frame model [8,9] |
| **Column web in shear** | EC3 [5] |
| **Stiffener in compression** | Proposed |
| **Bolts in tension** | EC3 [5] |
| **Bolts in shear** | EC3 [5] |
| **Lever arm** | Skejic et al. [12] |

*Table 4. Summary of approaches considered for the mechanical model.*

## 7. Effectiveness of mechanical proposal

The proposal is validated through comparison between the predicted and experimental results. Additional data were extracted from the experimental studies developed by Skejic et al. [12] and by Ghindea et al. [15]. The geometrical approximate values used to implement the stiffness coefficient $K_{sc}$ are shown in Table 5 with respect to Figure 15.

| | ST1 | ST2 | ST3-7 & Ghindea et al. | Skejic et al. |
|---|---|---|---|---|
| **H1** | 7 | 7 | 7 | 10 |
| **H2** | 74 | 72 | 70 | 72 |
| **Ls** | 99 | 97 | 95 | 132 |

*Table 5. Selected stiffener geometries (given in mm).*

Table 6 shows the comparative results considering the predicted and experimental rotational stiffness. The rotational stiffness prediction obtained yields with a mean value of 1.09 and a standard deviation of 0.06, showing good accuracy with respect to the tests used as a contrast in most cases. It also shows the advisability of using the lever arm proposal jointly with the non-aligned model and the choice of equivalent widths for stiffness calculations.

| Specimen | Kexp (kNm/rad) | Kpred (kNm/rad) | Kpred/Kexp |
|---|---|---|---|
| **ST1** | 6202 | 6655 | 1.07 |
| **ST2** | 6670 | 7112 | 1.07 |
| **ST3** | 7350 | 7436 | 1.01 |
| **ST4** | 6803 | 6712 | 1.04 |
| **ST5** | 6432 | 7143 | 1.05 |
| **ST6** | 5444 | 6056 | 1.11 |
| **ST7** | 4545 | 5158 | 1.13 |
| **ST8** | 5480 | 6024 | 1.10 |
| **B1** | 5014 | 5495 | 1.10 |
| **B2** | 4694 | 5495 | 1.17 |
| **C1** | 3859 | 4629 | 1.20 |
| **C2** | 3872 | 4629 | 1.20 |
| **D1** | 5455 | 5827 | 1.07 |
| **D2** | 5409 | 5827 | 1.08 |
| **TSDW10** | 7211 | 7346 | 1.02 |

| | | | |
|---|---|---|---|
| **TSS10** | 6978 | 6775 | 0.97 |
| | | **Mean** | **1.09** |
| | | **StDev** | **0.06** |

*Table 6. Comparison between predicted and experimental results for initial rotational stiffness.*

Although in the test program reported in this study, the component CWS does not develop deformation, it was considered in the general methodology description to extend the use of the method in cases where the deformational sources of this column component cannot be disregarded. In tests from Ghindea et al., the panel zone is not subjected to shear. Furthermore, Skejic et al. use an extremely rigid column for their experimental campaign, so the deformation is again negligible.

## 8. Discussion

The proposed methodology adapts to the Eurocode prescriptions, based on the Component Method, including all sources of deformation, because the significance of each component depends largely on the connection design. The Eurocode approach attempts to be a very open methodology, but this broad generalisation results in a complex approach, and even more so in the case of a connection that consists of so many components. However, the mechanical model regarding the Component Method is meant to be programmed, either in a sophisticated tool or in a simple spreadsheet, not solved by hand. On this basis, this complexity is partially dismissed.

From the comparison between the MR curves of tests *ST1–ST3*, corresponding to symmetrical stiffened top and seat angle joints with a double-web angle, the top and seat angle thickness increase leads to moderate rotational stiffness increments. In particular, the difference in stiffness between the *ST1* and *ST3* tests, with top and seat angle thicknesses of 8 and 10 mm, respectively, is 18.5%. This result contrasts with the values obtained in analogous tests with unstiffening top and seat angles [9], where the difference reached 39.4%. This comparison indicates that the effect on the initial stiffness of increasing top and seat angles thickness is reduced due to the presence of stiffeners.

In addition, the results of tests *ST5–ST7,* where the seat stiffened angle is the same but the configurations of the top and web angles are different, indicate a significant contribution of the web angle and the top angle stiffener to the joint stiffness. Considering the stiffness increase, the difference between tests *ST5* and *ST6* is 18%. In the

experimental study of Ghindea et al. [15], the difference in stiffness between tests TSDW10 and TSS10, with a 10 mm top and seat angle thickness, is only ~3%. This significant stiffness increase between tests *ST5* and *ST6* is probably due to the small thickness of the top and seat angles in these tests.

From the results of tests *ST3*–*ST5*, the effect of the isolated stiffened top angle thickness can be analysed. In this series, with the same stiffened seat angle, the initial rotational stiffness is similar, with marginal differences, but the effect on the resistance moment is large. Skejic et al. [12] pointed out that the stiffened seat cleat had the function of increasing the lever arm, while the stiffened top angle increased the bending resistance. The obtained results confirm the relevance of the stiffened top angle thickness in regards to resistance.

Considering tests *ST3* and *ST8*, the combined impact of the web angle and the stiffening of seat angle is analysed, resulting in a significant increase of the rotational stiffness. These outcomes are in concordance with the observations recorded by Skejic et al., where the stiffening of the seat angle had a large significance in the overall joint rotational stiffness [12]. In fact, the difference in stiffness between tests *ST3* and *ST8* is ~34%, similar to the difference value between series C and D from the work of Skejic et al., which is ~40%. In this sense, the experimental studies confirm the need to take into account the influence of the stiffener in the seat angle.

With regard to the stiffness values obtained through the proposed approach, the deviation is generally low, saving Skejic et al.'s *C* tests, with a stiffened top angle but an unstiffened seat angle. The results of the analytical model reflect values are, in almost all cases, higher than the experimental outputs. Since the EC3 method seems to overestimate the initial stiffness [12], the use of the EC3 mechanical model could explain, to a large extent, the results obtained. However, this study has followed alternative paths to the Eurocode to define many of the components, and, therefore, these results may also indicate the need to improve aspects of the model that are susceptible to a deeper analysis. In this sense, future works could focus on analysing in more depth the component stiffener in compression, trying to identify an effective width for the equivalent bar in compression. The lever arm proposed by Skejic et al. for joints with stiffened seat angle cleats, based on the analysis of experimental MR curves, seems to be an adequate approach in the absence of more specific studies. However, the mechanical model will probably be improved with a more accurate lever arm proposal, obtained by means of parametric studies on the influence of the different joint geometries. In contrast, the mechanical

proposal shows a good approximation for symmetrical configurations, which are the best choice to prevent reverse bending.

## 9. Conclusions

An experimental study composed of eight tests on stiffened angle joints has been carried out. The experimental study confirms the need to take into account the influence of the stiffener in the seat angle and the relevance of the stiffened top angle thickness as far as resistance is concerned. In addition, the effect on the initial stiffness of increasing top and seat angles thickness seems to be significantly reduced by the presence of stiffeners. A mechanical model, based on the Component Method of the Eurocode, for the prediction of the rotational stiffness of stiffened cleat angle joints is suggested. The proposal includes a recent plate model approach to reproduce the axial stiffness of stiffened angles in bending. In addition, the stiffener in compression is considered as a new component in the cases where the seat angle is stiffened. The proposed approach has been checked with experimental data from the developed tests and also from the literature, showing good agreement in almost all cases, in particular for symmetrical configurations. The lever arm proposed by Skejic et al. [12] for the characterization of joints with stiffened seat flange cleats has proved to be an acceptable approach ensuring, in general, good assessment of stiffness. Nevertheless, for a future study, the mechanical model will probably be improved by means of numerical parametric studies focussed on the influence of the geometrical properties, e.g. the gap between the beam and the column flange, in the location of the centre of compression, to obtain a more accurate definition of the lever arm.

## Acknowledgements

Financial support provided by the Spanish Ministerio de Economía y Competitividad and Fondo Europeo de Desarrollo Regional under contract BIA2016-80358-C2-2-P MINECO/FEDER UE is gratefully acknowledged.

## References


[1] M. Kidd, R. Judge, S.W. Jones, Current UK trends in the use of simple and/or semi-rigid steel connections. Case Studies in Structural Engineering, 6 (2016) 63–75. https://doi.org/10.1016/j.csse.2016.05.004

[2] D.D. Tingley, S. Cooper, J. Cullen, Understanding and overcoming the barriers to structural steel reuse, a UK perspective. Journal of Cleaner Production, 148 (2017) 642–652. https://doi.org/10.1016/j.jclepro.2017.02.006

[3] D.D. Tingley, B. Davison, Developing an LCA methodology to account for the environmental benefits of design for deconstruction, Building and Environment, 57 (2012) 387–395. https://doi.org/10.1016/j.buildenv.2012.06.005

[4] J.D. Schippers, D.J. Ruffley, G.A. Rassati, J.A Swanson, A design procedure for bolted top-and-seat angle joints for use in seismic applications. 7th International Workshop on joints in steel structures, Timisorara, 2012.

[5] EUROCODE 3, Design of Steel Structures – part 1.8: Design of joints CEN, Brussels, 2005.

[6] A. Azizinamini, J.H. Bradburn, J.B. Radziminski, Initial Stiffness of Semi-Rigid Steel Beam-to-Column Joints. Journal of Constructional Steel Research, 8 (1987) 71–90. https://doi.org/10.1016/0143-974X(87)90054-X

[7] C. Faella, V. Piluso, G. Rizzano, Structural Steel Semirigid Joints. CRC Press LLC, Boca Ratón, Florida, 2000.

[8] A. Loureiro, J.M. Reinosa, R. Gutierrez, A. Moreno, Axial stiffness prediction of non-preloaded T-stubs: An analytical frame approach. Journal of Constructional Steel Research, 66 (2010) 1516–1522. https://doi.org/10.1016/j.jcsr.2010.06.005

[9] J.M. Reinosa, A. Loureiro, R. Gutierrez, M. Lopez, Analytical frame approach for the rotational stiffness prediction of beam-to-column angle connections. Journal of Constructional Steel Research, 106 (2015) 67–76.
https://doi.org/10.1016/j.jcsr.2014.12.005

[10] M.E. Lemonis, C.J. Gantes, Mechanical modelling of the nonlinear response of beam-to-column joints. Journal of Constructional Steel Research, 65 (2009) 879–890.
https://doi.org/10.1016/j.jcsr.2008.11.007

[11] A.M. Citipitioglu, R.M. Haj-Ali, D.W. White, Refined 3D Finite element modeling of partially-restrained joints including slip. Journal of Constructional Steel Research, 58 (2002) 995–1013. https://doi.org/10.1016/S0143-974X(01)00087-6

[12] D. Skejic, D. Dujmovic, D. Beg, Behaviour of stiffened flange cleat joints. Journal of Constructional Steel Research, 103 (2014) 61–76. https://doi.org/10.1016/j.jcsr.2014.07.011

[13] J.M. Reinosa, A. Loureiro, R. Gutierrez, M. Lopez, Analytical plate approach for the axial stiffness prediction of stiffened angle cleats. Journal of Constructional Steel Research, 106 (2015) 77–88. https://doi.org/10.1016/j.jcsr.2014.12.010

[14] D. Skejic, D. Dujmovic, I. Lukacevic. Unstiffened and stiffened cleats under bending: Experimental investigation. Eurosteel 2011. Budapest. Volume A: 309–314.

[15] M. Ghindea, A. Catarig, R. Ballok, Behavior of Beam-to-Column Joints with Angles. Part 1- Experimental Investigations, Journal of Applied Engineering Sciences, 18 (2015) 21–28.

[16] D. Skejic, D. Beg, D. Dujmovic, Beam-to-Column Joints with Stiffened Flange Cleats. Experimental Investigation. Eurosteel 2014. Naples. Abstracts book: 375–376

[17] J.M. Reinosa, A. Loureiro, R. Gutiérrez, M. López., Estudio experimental y numérico de uniones con angulares ejecutadas con perfiles europeos. Informes de la Construcción, 66 (2014) Extra1.